

Stable isotope characteristics of precipitation of Pamba River basin, Kerala, India

T R RESMI*, K V SUDHARMA and A SHAHUL HAMEED

Isotope Hydrology Division, Centre for Water Resources Development and Management, Kunnamangalam P O, Kozhikode, Kerala 673 571, India.

**Corresponding author. e-mail: rtr@cwrdm.org*

Stable isotope composition of precipitation from Pamba River basin, Kerala, India, is evaluated to understand the role of spatial and temporal variations on rainwater isotope characteristics. Physiographically different locations in the basin showed strong spatial and temporal variations. $\delta^{18}\text{O}$ varied from -7.63 to -1.75‰ in the lowlands; from -9.32 to -1.94‰ in the midlands and from -11.6 to -4.00‰ in the highlands. Local Meteoric Water Lines (LMWL) for the three regions were determined separately and an overall LMWL for the whole of the basin was found to be $\delta^2\text{H} = 6.6 (\pm 0.4) \delta^{18}\text{O} + 10.4 (\pm 2.0)$. Altitude effect was evident for the basin (0.1‰ for $\delta^{18}\text{O}$ and 0.8‰ for $\delta^2\text{H}$ per 100 m elevation), while the amount effect was weak. The precipitation formed from the marine moisture supplied at a steady rate, without much isotopic evolution in this period may have masked the possible depletion of heavier isotopes with increasing rainfall. Consistently high d-excess values showed the influence of recycled vapour, despite the prevailing high relative humidity. The oceanic and continental vapour source origins for the south-west and north-east monsoons were clearly noted in the precipitation in the basin. Rayleigh distillation model showed about 30% rainout of the monsoon vapour mass in the basin.

1. Introduction

Isotope techniques have proved to be a powerful tool for solving many intricate problems in hydrological research. Understanding the formation mechanism and process modifications undergone by the different components of the hydrological cycle is important in basin-scale water resources management (Vreča *et al.* 2006). Information on the isotopic composition (δD and $\delta^{18}\text{O}$) of precipitation and its spatial and temporal variations are vital inputs in river basin hydrology. The isotopic composition of local precipitation is controlled by regional scale processes such as the weather condition at the origin of the vapour source, the trajectory of water vapour transport and the rainout history of the air mass that results in precipitation

at a particular time and place (Rozanski *et al.* 1982; Aragus-Aragus *et al.* 2000). The relationship between $\delta^2\text{H}$ and $\delta^{18}\text{O}$ in fresh surface waters is defined as $\delta^2\text{H} = 8 \delta^{18}\text{O} + 10\text{‰}$ SMOW by Craig (1961) is known as the global meteoric water line (GMWL). Later, Rozanski *et al.* (1993) redefined this equation to $\delta^2\text{H} = 8.17 (\pm 0.07) \delta^{18}\text{O} + 11.27 (\pm 0.65)\text{‰}$ VSMOW by measuring the δD and $\delta^{18}\text{O}$ of precipitation samples only. The relationship can vary from region to region making it an advantage to establish a local meteoric water line (LMWL), specific to the study area (Simpkins 1995; Gammons *et al.* 2006; Gupta and Deshpande 2003, 2005; Rhodes *et al.* 2000; Wassenaar *et al.* 2011; Hu *et al.* 2013; Hunjak *et al.* 2013; Stumpp *et al.* 2014).

Important information that can be gathered by isotope ratio analysis of precipitation samples

Keywords. Isotope ratio; precipitation; spatiotemporal variation; statistics; tropical river basin.

involves primary and secondary processes that control the evaporation–condensation cycles in a particular region (Yang *et al.* 2013). The formation of precipitation begins with the evaporation of water from the oceans, the evolution of δD and $\delta^{18}O$ composition of meteoric waters also begins with the same process. The rate of evaporation limits vapour–water exchange and so consequently the degree of isotopic equilibrium between the two phases (Gupta and Deshpande 2003, 2005). Isotopic equilibrium is attained if the evaporation and condensation fluxes are same and increased rate of evaporation imparts a kinetic or non-equilibrium isotope effect on the vapour. Surface temperature, wind speed, salinity and most importantly, humidity are the factors influencing kinetic isotope effect. At lower humidity, water–vapour exchange across the boundary layer becomes increasingly unidirectional (water to air), and evaporation becomes increasingly a non-equilibrium process (Gupta and Deshpande 2003, 2005). The behaviour of 2H and ^{18}O in the hydrosphere is intimately linked to the mechanism prevailing during cloud and precipitation formations. During the formation of cloud by the cooling of moist air, isotopic equilibrium is attained if the vapour condenses to form droplets. However, kinetic fractionation is also possible if the vapour directly transforms to ice crystals (Fritz and Fontes 1986). Once the drops and/or ice crystals coalesce to form precipitation, the isotopic composition is again modified during its journey through the air column to the ground. Evaporation from the rain drops and exchange with environmental vapour are important for the final composition of liquid precipitation reaching the ground (Dansgaard 1964). The rainout history of the air parcel also affects the isotopic composition of the precipitation occurring in a particular region.

The state of Kerala is located on the south-western tip of the Indian subcontinent, positioned directly across the path of the maritime air blowing from the Indian Ocean and the Arabian Sea during the northern hemispheric summer (Menon and Rajan 1989). The moist air undergoes orographic lift by the Western Ghats mountain series. Studies on the effect of orography in isotope composition of rainwater in the Kerala region, where the monsoon strikes first in the subcontinent, are very scanty (Deshpande *et al.* 2003; Gupta *et al.* 2005; Warriar *et al.* 2010). In this paper, the Pamba River basin, situated in the humid tropics of Kerala, India, was investigated for temporal and spatial variations in the isotopic composition of precipitation in order to identify the meteorological controls on it. By characterising the stable isotope distribution in precipitation of the river basin, a highly essential input function for isotope hydrology studies is determined. The information can

be used to identify the provenance and recharge mechanism of groundwater in the basin, facilitating the management strategies.

2. Study area

The Pamba River basin lies between $09^{\circ}10'$ and $09^{\circ}37'N$ latitudes and $76^{\circ}19'$ and $77^{\circ}08'E$ longitude. The river rises in the Peerumedu Plateau at an elevation of 1670 m (AMSL). The basin lies entirely in the Kerala State (Pathanamthitta, Idukki, and Alappuzha districts) and the total catchment area is 2235 km², up to the confluence with the Vembanad estuary. The mainstream Pamba, 176 km in length, is the third longest river in Kerala and is formed by the confluence of the Pamba Ar, Kakki Ar, Azhutha Ar, Kakkad Ar, and Kall Ar. Physiographically, Kerala is divided into the lowlands (<7 m), the midlands (7–75 m) and the highlands (>75 m) above mean sea level (AMSL). The same classification holds good for the Pamba River basin also. The upper reaches (highlands) of the basin are made up of crystalline rocks of Precambrian. The midlands are mostly covered by laterite and the lowlands comprise of recent alluvium and beach sands. The drainage map with sample locations of the basin is given in figure 1. The land use of the basin is dominated by forest (52.4%) and the rest 25.4% by plantations (rubber, coconut, teak, tea, etc.), 16.3% by agriculture, and 5.9% by fallow lands.

2.1 Climate

The Pamba River basin experiences ~ 3000 mm of rainfall per year. The south-west and north-east monsoons have great influence over the climatic conditions. Average annual rainfall varies from 2276 mm near the coast (lowland) to 4275 mm in the highlands. The relative contribution of south-west monsoon (June–September), north-east monsoon (October–December) and pre-monsoon rainfall (January–May) in the basin are 56.8%, 21.7% and 21.5%, respectively (CWC 2006).

The rainfall distribution in the Pamba basin is mainly influenced by the geographical disposition and the physical features within the basin. The Western Ghats forming the eastern boundary of the basin receives high rainfall ranging from 3659 to 4307 mm. The areas west of the Western Ghats receive lesser rainfall (~ 2800 mm) with increasing distance from the Western Ghats (NWDA 2008). According to a study by Mayaja and Srinivasa (2014), the annual rainfall in the highland area of the basin is about 10–30% higher than the state average. Further, by analysing the trend of long-term monsoon data, they found that the highlands

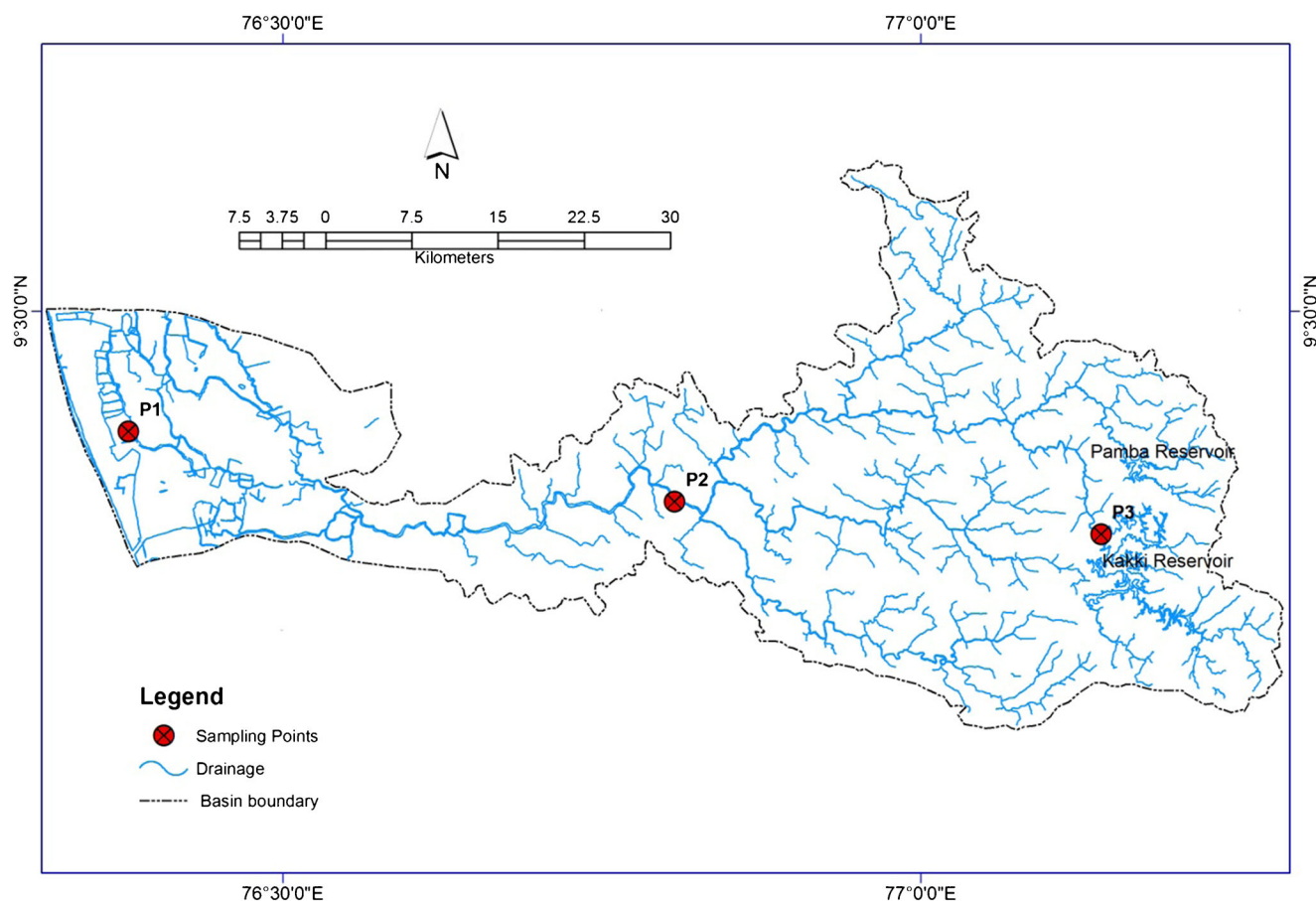


Figure 1. Drainage map of Pamba River basin with sampling locations.

show a positive trend during the south-west monsoon, and in the other seasons the trend remains more or less stable. In contrast to the highlands, rainfall pattern in the midland and lowland regions show a homogeneous negative trend during the south-west monsoon and north-east monsoon periods and remain more or less stable during the pre-monsoon.

The basin experiences moderate temperature (daily temperature varies between 22.6° and 32.7°C). Near the coast, diurnal and seasonal variation is in the range 5°–7°C due to marine influence. However, due to orographic effect, diurnal variation in temperature is very high in the highlands (>15°C) (CWRDM 1995). Diurnal variation is least in the month of July, because the skies are mostly overcast and the duration of sunshine is comparatively short (Menon and Rajan 1989).

The relative humidity varies from 53 to 95% in the Pamba River basin (CWC 2006). Except during the monsoon months, relative humidity is low (53–75%) (NWDA 2008). The coastal area has a high percentage of humidity and it diminishes progressively towards the Western Ghats (Madhusoodhanan *et al.* 2012). Relative humidity is lowest in the afternoon and highest during morning hours. Wind

speed in the Pamba River basin varies from 8.5 to 13.6 km/hr (NWDA 2008). Large diurnal variation in winds at the surface and the layers immediately above is a characteristic feature of the coastal regions where the effect of land and sea breeze is predominant. However, during the south-west monsoon, when the prevailing winds are from the sea to land throughout, the sea breeze gets superimposed on the prevailing wind. In the interior and over hilly terrain, diurnal variation is mainly determined by the topography. In the mountainous regions, there are mountain and valley winds. During daytime, winds are going up the slopes (anabatic winds) and during night, there is down-slope or katabatic flow (Menon and Rajan 1989).

Studies on evapotranspiration in the Pamba River basin are not available and hence, for the present study, data for entire Kerala state and water demand for crops computed for each district is used. Since physiography of the districts is similar and the agricultural practices are same, the collected data can be applied for the Pamba River basin also. Thus, the evapotranspiration demand of the state is estimated to be above 1000 mm annually (Gordon *et al.* 2005). During all seasons, elevated regions over the Western Ghats experience

much lower water needs compared to the plains inside Kerala State (Saravanan 1994). Distribution of potential evapotranspiration values is uniform in the coastal tracts while there are a few pockets of low values in the hill stations of the Ghats region. Lowland and midland areas have comparatively high potential evapotranspiration values (>170 cm). The lowest values of annual potential evapotranspiration (<90 cm) are seen over Anamalai hills. Maximum normal monthly potential evapotranspiration occurs in May and the lowest in February or July (James 1991). The reference crop evapotranspiration (ET_0) computed is 1467 mm per year (Surendran *et al.* 2014). The water requirement (ET_C) calculated for different crops under different agro-ecological units of Kerala is as follows: Rubber – 1366 mm, Coconut – 1094 mm, Tea – 1286 mm, Tapioca – 800 mm. Pepper – 981 mm and Paddy – 1565 mm (Surendran *et al.* 2014).

As mentioned earlier, almost half of the area of the basin is covered by forests and the quarter of the area by plantation crops like rubber, coconut, teak, tea, etc. In the lowland region of the basin, paddy is the main agriculture crop. The effect of conversion of natural forests to plantation crops especially, rubber plantations on water yield has been studied extensively. Soman *et al.* (1988) found that rainfall in south Kerala has decreased significantly during the 40-year period, 1941–1980, compared to the preceding 40 years from 1901 to 1940. They have attributed this phenomenon to deforestation and replacement of natural vegetation by rubber. It was also reported that water flow in the rivers flowing through these tracts is reducing. According to Celine and James (2015), a 50% increase in area under rubber plantation reduced water yield by 9.6%, surface runoff by 12.8% and increased evapotranspiration by 3.3% in the nearby Achankovil basin. In the rubber plantations of Kerala, Chattopadhyay (2015) found that the water use by rubber is 500–600 mm lower than typical tropical rain forest ecosystem and the rate of evapotranspiration was lower for rubber plantation compared to the forest ecosystem.

2.2 Sampling and analytical techniques

Monthly composite precipitation samples from the Pamba River basin were collected according to the physiographic classification. Location code P1 stands for the lowland region (actual elevation 3 m AMSL), P2 for the midlands (65 m AMSL) and P3 for the highlands (968 m AMSL). In the lowland region, the river drains into the Vembanad estuary through numerous channels in Kuttanad, and the entire area is criss-crossed by drainage channels of four other rivers also. The midland region is characterised by plantations like rubber, coconut,

areca nut, paddy and other cash crops. The highland region is covered by dense forests and the sampling point is adjacent to the second largest reservoir for the hydroelectric power production in the state.

Precipitation samples were collected in 20 L plastic carboys specially designed to reduce evaporation. A funnel with large diameter (21 cm) was used to collect the precipitation. A thick plastic tube was connected to the stem of the funnel, which reaches up to the bottom of the carboy. Another thick plastic tube of internal diameter 0.5 mm and length 5 m was connected in the mouth of the carboy to facilitate overflow of the sample, if in excess of the capacity of the sampling bottle. The funnel and the outer tubing were fitted into a nylon thread in the mouth of the carboy. The monthly composite samples collected in this way were later sub-sampled to high-density polyethylene bottles (60 mL capacity) for isotope measurement in the laboratory. Utmost care was taken not to trap any air bubble inside. The samples were measured for oxygen and hydrogen isotope ratio and the data are presented in table 1. Water samples for oxygen isotope analysis were prepared by H_2O-CO_2 equilibration technique (Epstein and Mayeda 1953). About 200 μ L of each sample was equilibrated with laboratory standard CO_2 gas at 30°C. Hydrogen isotope was analysed by the equilibration with standard H_2-He gas mixture in the presence of Pt catalyst coated on hydrophobic polymer. Both the isotopes were measured using the Continuous Flow Finnigan Delta Plus^{XP} Isotope Ratio Mass Spectrometer with reference to the standard V-SMOW. The analytical reproducibility is $\pm 0.18\text{‰}$ for $\delta^{18}O$ and $\pm 1.8\text{‰}$ for δD . The results were expressed in δ values as:

$$\delta = \left[\frac{R \text{ sample}}{R \text{ standard}} - 1 \right] \times 1000,$$

where R represents either $^{18}O/^{16}O$ or D/H ratio.

Meteorological data like, daily minimum and maximum temperature, daily minimum and maximum relative humidity and amount of rainfall were collected for all the three locations.

3. Results and discussion

3.1 Statistical analysis

$\delta^{18}O$ of rainwater varied from -7.63 to -1.75‰ in the lowlands; from -9.32 to -1.94‰ in the midlands and from -11.6 to -4.00‰ in the highlands. δD ranged from -42.0 to -1.89‰ in the lowlands; from -52.7 to -6.22‰ in the midland and from -70.6 to -11.5‰ in the highland region. The general statistics of the isotope data shows

Table 1. Stable isotope data of precipitation in the Pamba river basin.

	$\delta^{18}\text{O}$ (‰)	δD (‰)	d-excess (‰)
Lowland			
September 09	-3.49	-16.5	11.5
January 10	-7.63	-42.0	19.1
April 10	-1.75	-1.89	12.1
May 10	-2.09	-2.79	13.9
July 10	-3.34	-13.6	13.1
October 10	-6.28	-34.4	15.8
November 10	-5.28	-20.4	21.8
March 11	-6.93	-30.1	25.4
Max	-1.75	-1.89	25.4
Min	-7.63	-42.0	11.5
Mean	-4.60	-20.2	16.6
Std. Dev.	2.24	14.5	5.02
Midland			
September 09	-2.99	-12.1	11.8
January 10	-9.32	-52.7	21.9
April 10	-1.94	-11.0	13.6
May 10	-2.73	-7.18	14.7
July 10	-3.2	-6.22	19.4
October 10	-6.12	-36.0	12.9
November 10	-6.71	-28.1	25.6
March 11	-5.68	-20.8	24.6
Max	-1.94	-6.22	25.6
Min	-9.32	-52.7	11.8
Mean	-4.84	-21.8	18.1
Std. Dev.	2.53	16.3	5.51
Highland			
September 09	-4.32	-18.2	16.4
January 10	-11.6	-70.6	22.1
April 10	-4.90	-22.7	28.2
May 10	-4.00	-11.5	20.5
July 10	-4.13	-16.7	16.3
October 10	-6.19	-33.6	15.9
November 10	-7.71	-41.8	19.8
March 11	-5.61	-19.2	25.7
Max	-4.00	-11.5	28.2
Min	-11.6	-70.6	15.9
Mean	-6.06	-29.3	20.6
Std. Dev.	2.56	19.3	4.55

that standard deviation was highest for samples collected from the highland region, followed by the midlands and lowest for the lowland region. Since the standard deviation was high among the samples, two-factor analysis of variance (ANOVA) without replication was done to find out the significant spatiotemporal variation in isotopic composition (table 2). ANOVA was carried out on δD and $\delta^{18}\text{O}$ with respect to months and locations. Even though the variations were significant spatially and temporally, the temporal variation in stable isotope composition of precipitation in the river basin was more significant than spatial.

3.2 Distribution of δD and $\delta^{18}\text{O}$

3.2.1 Spatial

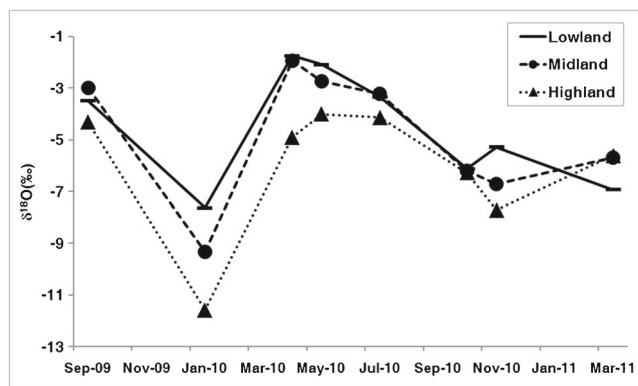
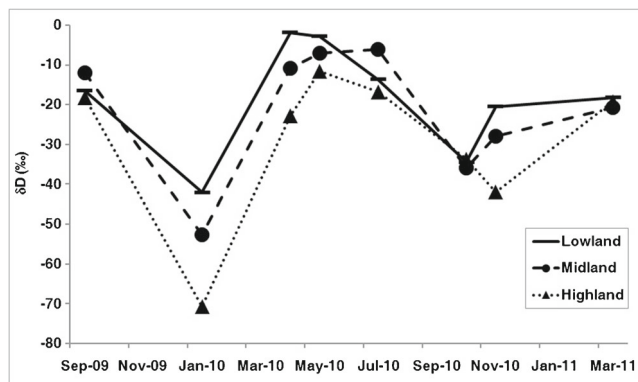
The δD and $\delta^{18}\text{O}$ values exhibited a similar distribution pattern in the lowland, midland and highland regions of the basin (figures 2 and 3). A relatively enriched isotopic composition was recorded in the precipitation of the lowland region than those of the midland and highland regions. The highland precipitation was found to be most depleted throughout the year. The three sampling locations are situated at different elevations (3, 65 and 968 m AMSL) according to the physiography of the basin. Depletion of heavier isotopes in precipitation with respect to elevation/altitude is well known (Cortes *et al.* 1997; Garcia *et al.* 1998; Gonfianitini *et al.* 2001; Guan *et al.* 2009; Kattan 2006; Scholl *et al.* 2009; Vuille *et al.* 2005; Brietenbach *et al.* 2010; Kumar *et al.* 2010; Peng *et al.* 2010; Windhorst *et al.* 2013). In Kerala, even though the areal distance between the lowland near the coast and highland mountain ranges is relatively small (~120 km), isotopic modifications are manifested in the precipitation samples due to the orographic uplift of the monsoon air mass. The Western Ghats has undulating topography, with two peaks in the southern (Anamudi 2699 m) and northern sides (Doda Betta 2644 m) and a gap of length 24 km (Palghat Gap) almost near the centre. The Peerumedu Plateau (1067 m), from where the Pamba River originates, is on the southern offshoot from the Anamudi Peak. The forced ascent of the air mass on the windward side of the mountains gives copious rain (~3500 mm). In accordance with the increasing elevation, heavier isotopes are progressively depleted in the precipitation or we can say that the altitude effect is clearly visible in the precipitation over the Pamba River basin.

The altitude effect in successive precipitation is basically a temperature dependent phenomenon and is explained on the basis of adiabatic cooling related rainout process. The adiabatic cooling refers to the change in temperature of a mass of air as it moves upward in the atmosphere. The lapse rate varies significantly with the amount of moisture content of the air mass. The altitude effect is expressed often as an isotopic lapse rate and given as per mil (‰) change in $\delta^2\text{H}$ and $\delta^{18}\text{O}$ of precipitation per 100 m of elevation change. Most of the reported lapse rate for $\delta^{18}\text{O}$ and $\delta^2\text{H}$ lie in the range of -0.1 to -0.6‰ per 100 m and -0.5 to -4‰ per 100 m, respectively. In the Kumaon Himalayas of India, Kumar *et al.* (2010) reported a depletion of -0.36‰ and -2.61‰ for $\delta^{18}\text{O}$ and $\delta^2\text{H}$, respectively, per 100 m elevation.

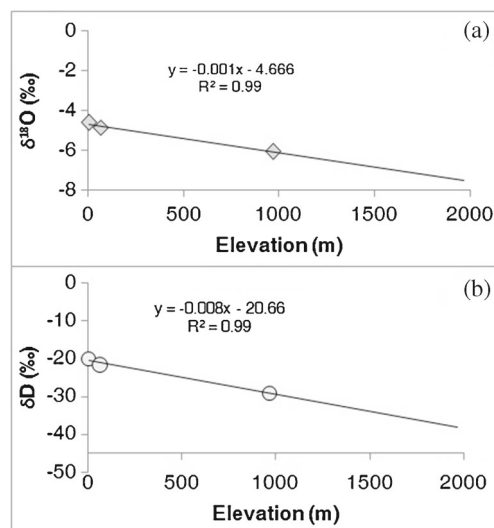
The average δD and $\delta^{18}\text{O}$ values of precipitation of the Pamba River basin plotted against the

Table 2. Analysis of variance (two factor without replication) of isotope data of precipitation in the Pamba river basin.

Source of variation	Sum of squares	Degrees of freedom	Mean squares	F	P-value	F critical
$\delta^{18}\text{O}$						
Month	114.052	7	16.29314	19.46	3.35E-06	2.764
Location	9.766458	2	4.883229	5.831	0.014382	3.739
Error	11.72408	14	0.837434			
Total	135.5425	23				
δD						
Month	5271.851	7	753.1215	15.95	1.12E-05	2.764
Location	388.7662	2	194.3831	4.116	0.039275	3.739
Error	661.2079	14	47.22914			
Total	6321.825	23				
d-excess						
Month	314.1236	7	44.8748	0.702	0.670576	2.764
Location	94.8199	2	47.40995	0.742	0.493954	3.739
Error	894.4425	14	63.88875			
Total	1303.386	23				

Figure 2. Spatial and temporal variation of $\delta^{18}\text{O}$ of precipitation in the Pamba River basin.Figure 3. Spatial and temporal variation of δD in precipitation of Pamba River basin.

elevation of their sampling sites are given in figure 4(a and b). Altitude effect for $\delta^{18}\text{O}$ is 0.1‰ per 100 m elevation and for δD , it amounts to 0.8‰ per 100 m elevation in precipitation of Pamba River basin. In this investigation, no change in altitude effect, in different seasons, is observed in the basin. Hence, it can be assumed that the main driving force of altitude effect in the basin is

Figure 4. Variation of $\delta^{18}\text{O}$ and δD of precipitation with elevation (altitude effect) of Pamba River basin.

the temperature induced rainout process. Local climatic factors are distinctly different for the three regions in the study area. The highlands are characterised by low air temperature and dense rainforests, whereas the lowlands lie near the coast and are surrounded by large surface water bodies. The cooler air temperature in the highlands and the rainout process might have resulted in depleted isotopic composition of the precipitation.

3.2.2 Temporal

On examination of the monthly variation of isotope composition of precipitation, it was noted that the δ values were lowest in the month of November and highest during the summer rains, at all locations. In the study area, the south-west monsoon begins in the middle of May and extends up to September.

The winds start retreating from the continent in the month of October and being in the rain shadow region of the retreating monsoon winds (north-east monsoon), the area receives precipitation depleted in heavier isotopes during November to January ($\delta^{18}\text{O} = -3.58\text{‰}$ during south-west monsoon and -7.43‰ in north-east monsoon). Schmidt *et al.* (2007) and Sturm *et al.* (2007) have found that the altitude effect is more important in areas that contain orographic barriers. Besides, it has been recorded, earlier in Kerala, that the north-east monsoon is isotopically depleted (-7.3‰) than the south-west monsoon (-2.8‰), probably because of the difference in vapour source origins; the first being continental and the other oceanic (Warrier *et al.* 2010).

Summer rains are occasional in Kerala, with large regional variability. They are characterised by high thunderstorm activity. During the pre-monsoon season, intense heating of the ground results in high convection, formation of cumulonimbus clouds and thereby thunderstorm activities (Pradeep Kumar 1994). In large thunder clouds, the water droplets have to undergo several cycles of evaporation and condensation and they are subjected to vertical transport many times inside the cloud. The evaporation–condensation cycles at the sub-zero level often lead to the formation of ice crystals, and isotopic fractionation occurs in three stages inside a thunder cloud. These are: (i) equilibrium isotope fractionation between the droplets and vapour, (ii) kinetic fractionation between ice crystals and vapour and (iii) isotopic exchange between large drops and vapour (Fritz and Fontes 1986). The first stage, equilibrium isotope fractionation between the droplets and vapour occurs at the initial stages of cloud formation. For a droplet evolving in a cloud where environmental conditions such as air pressure, temperature and isotopic content of water vapour are continuously modified, a radius of less than 30 μm can be considered to be in isotopic equilibrium with the vapour, irrespective of cloud conditions and stage of droplet formation. The second stage of kinetic fractionation is between the ice crystals and vapour. Once the cloud extends to an altitude above 0°C isotherm, ice crystals will form by two types of phase transitions: the complete freezing of a liquid droplet or the direct deposition of vapour onto the solid phase. No isotopic fractionation occurs if ice is formed by the complete freezing of the liquid droplet. Ice formed by direct condensation of vapour grows in isotopic equilibrium with the vapour. However, the growth includes a diffusion process of the vapour through a supersaturated environment. Thus, kinetic isotopic fractionation leads to an isotopic enrichment in the ice. The third stage of isotopic fractionation

in the clouds is the isotopic exchange between large drops and vapour. Large liquid drops, which are not in isotopic equilibrium with water vapour, will be enriched in heavy isotopes with respect to cloud droplets at the same temperature. Thus the isotopic composition of the rain drops that leaves from the cloud base is remarkably different from the up-drafting incoming air.

In addition to this, the summer or the pre-monsoon period (February–May) are the hottest months and the precipitation occurring at this time encounters a high temperature difference between the cloud base and the ground level. This phenomenon facilitates evaporation on the falling rain drops and the precipitation finally reaching the ground may be enriched in heavier isotopes (secondary fractionation). For the present investigation, cloud base height (CBH) was calculated according to the Bradbury rule (Croucher 2007). The CBH was calculated using the formula

$$\text{Spread} = \text{Surface air temperature} - \text{Dew point.}$$

$$\text{CBH(AMSL)} = (\text{spread} \times 400)$$

$$+ \text{Ground elevation in AMSL.}$$

Analysis of the cloud base height (CBH) at the lowland and midland regions during two consecutive years of sampling showed that at both the regions, the pre-monsoon period is characterised by the highest CBH from the ground level as well as from AMSL (figure 5). CBH was lowest during the monsoon months and showed an increasing trend in the post-monsoon period. As mentioned earlier, the surface temperature is highest and relative humidity is lowest in the pre-monsoon season in the Pamba River basin. Thus, the precipitation formed during the pre-monsoon period has to travel a relatively longer distance with a high temperature gradient between the cloud base and ground level through less humid air column

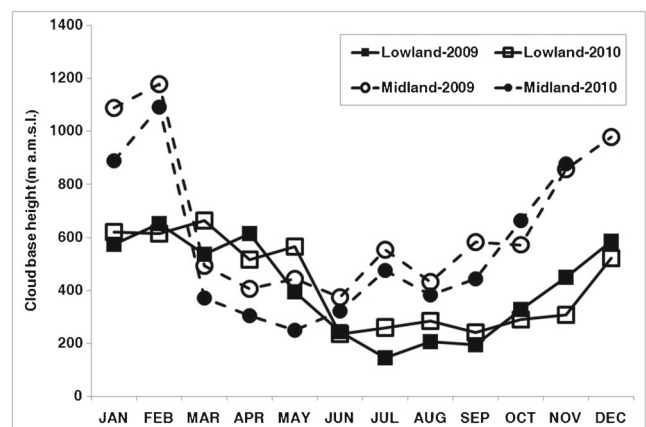


Figure 5. Monthly variation of cloud base height (CBH) at the lowland and midland regions of the Pamba River basin.

when compared to the other two seasons. Accordingly, secondary fractionation on the falling rain drops is more pronounced in this season resulting in isotopically enriched precipitation.

However, it may be noted that the δ values of the three regions were similar especially in the month of September in 2009 and October in 2010. These two months can be considered as the retreating phase of the south-west monsoon season and the precipitation may have acquired a uniform isotopic composition. Similarly, large variation in δ values was observed in the month of January, the coldest month. The temperature gradient for the three regions was high during this month (see section 2.1), and accordingly, the rate of secondary evaporation of the rain drops may be different at the three regions causing different isotopic composition.

The area receives the highest rainfall during the south-west monsoon season especially during the month of July (~ 350 mm). Still, a corresponding depletion in heavier isotope with increased rainfall amount could not be observed in any of the three locations selected for this study. The onset of south-west monsoon in Kerala is in June. As indicated by Soman and Krishna Kumar (1993), the build-up of moisture occurs a few days prior to the onset. The prevailing winds during the onset of the monsoon are westerly from the surface to about 6 km and blow from the sea to the land. By July, the monsoon is established fully over the entire state. The westerlies are steady and fairly strong (20–30 kt). Under strong monsoon conditions, the westerlies increases in strength, often reaching 60 kt or more, at about 1.5 km. Other meteorological parameters, like relative humidity, temperature, cloudiness, etc., are almost similar during this time over the entire study area. Precipitation formed from the air mass under similar meteorological conditions can be assumed to be the reason for the negligible variation in isotopic composition in July. In other words, the influence of the amount effect on the relationship between $\delta^{18}\text{O}$ and temperature is very poor.

3.3 Local meteoric water lines (LMWL)

Craig (1961) first defined the relation between hydrogen and oxygen isotopes in meteoric waters, generally known as the ‘Global Meteoric Water Line’ (GMWL), as $\delta^2\text{H}=8 \delta^{18}\text{O}+10$. Later Rozanski et al. (1993) reported an empirical regression line for the long term annual weighted mean of δD and $\delta^{18}\text{O}$ values collected in the Global Network of Isotopes in Precipitation (GNIP) as:

$$\delta^2\text{H} = 8.20 (\pm 0.07) \delta^{18}\text{O} + 11.27 (\pm 0.65).$$

This line is actually an average of many local meteoric water lines (LMWL) that differ from the global line in both slope and intercept, in accordance with the varying climatic and geographical parameters.

The LMWLs computed separately for the lowland, midland and highland regions of the Pamba basin is given in figure 6. The precipitation samples in the three regions were found to plot above the GMWL indicating the importance of recycled vapour in characterising the isotopic composition of the precipitation in the basin. As stated earlier, the lowland region of the Pamba River basin supports large surface water bodies. The Vembanad Estuary, into which Pamba along with four other large rivers drains, is the largest estuary of the state (area = 2133 km²) and is considered to be the longest in the country (Gopakumar and Takara 2009). Most the lowland area of the basin is under paddy cultivation in large extents and is submerged most part of the year. In the case of midlands, the region is dominated by plantation crops and as a consequence, vapour from the irrigated water as well as the vapour from evapotranspiration of the crops may have modified the isotopic composition of the ambient vapour in that region. The vapour formed by the evaporation of the irrigated water will be somewhat depleted in heavier isotopes, whereas the transpiration returns essentially isotopically unfractionated water to the atmosphere (Zimmerman et al. 1967), despite the complex fractionation processes in leaf water (Forstel 1982). In other words, evaporated vapour is usually depleted in heavier isotopes relative to that of transpired vapour and is actually closer to the composition of the atmospheric vapour. The highland area of the basin is marked by large reservoirs formed by the Pamba, Kakki, Anathodu, Moozhiyar, Maniyar and Kakkad Ar dams. Most of these reservoirs are for power generation, while a few are for irrigation. Contribution

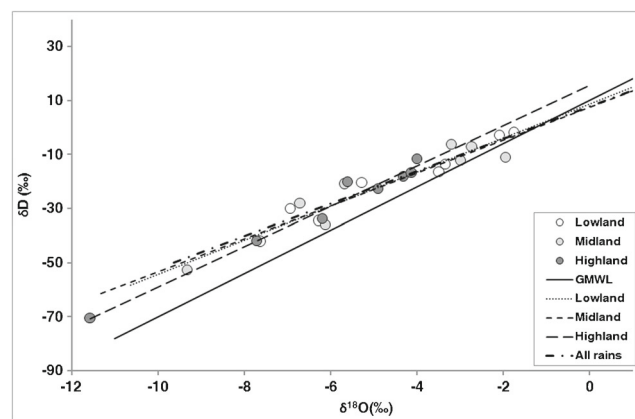


Figure 6. Regression plot of δD vs. $\delta^{18}\text{O}$ of precipitation in different regions of the Pamba River basin. Regression line for all rains are also provided.

from recycled/evaporated vapour from these areas and surface water bodies is significant to the ambient vapour, modifying the isotopic composition of precipitation.

The regression parameters for the individual regions and the combined values for the entire basin are provided in table 3. All the three regression lines were plotted close to the GMWL, but with different slopes and intercept values. The lowering of the slope value below eight indicates the evaporative enrichment of heavier isotopes in the falling rain drops. Among the three regions, the slope and intercept were lower for the lowland (6.3 ± 0.6) and midland (6.1 ± 0.9) regions, than the highland region (7.5 ± 0.5). The relative higher slope and intercept values obtained for the highland location can be due to the cumulative effect of higher elevation, lower air temperature and the influence of reservoir water vapour. Secondary fractionation leading to enrichment of heavier isotopes in the falling raindrops may be relatively lesser at this location due to the low air temperature and can result in relatively higher values of slope than the lowland and midland regions. However, the higher intercept value may indicate precipitation from rather rained out air mass. Most depleted $\delta^{18}\text{O}$ values obtained for this region also corroborates with the above observation. For the lowland and midland regions, the slope as well as y-intercept values were closer (lowland: $s = 6.3$, y-intercept = 8.8; midland: $s = 6.1$, y-intercept = 7.7). In figure 6, it can be seen that the scatter is relatively less for the lowland and midland precipitation δ values than highland. The slope, as well as the y-intercept obtained for these regions, may be representing the first condensate from the monsoon air mass without much isotopic evolution. A possible reason for the slope value being <8 is due to evaporation from the falling rain drops, as seen in the foregoing section. Since the lowland station is very close to the sea, relative humidity is higher than those of the highlands. However, a slope value of 6.3, at this station, points to the extent of evaporation occurring in the precipitation, once it leaves the cloud base, may be due to the high surface air temperature.

The overall local meteoric water line for the Pamba basin proposed is as follows:

$$\delta^2\text{H} = 6.6 \pm 0.4 \delta^{18}\text{O} + 10.4 \pm 2.0.$$

Table 3. Regression parameters of precipitation in different topographic regions in the Pamba River basin.

Region	Slope (m)	Y-intercept	R^2
Lowland	6.3 ± 0.6	8.8 ± 3	0.949
Midland	6.1 ± 0.9	7.7 ± 4.7	0.892
Highland	7.5 ± 0.5	15.7 ± 3.1	0.977
All rains	6.6 ± 0.4	10.4 ± 2	0.939

3.4 Deuterium excess (d-excess)

The slope of GMWL is determined by the ratio between the equilibrium fractionation effects of hydrogen and oxygen, while the intercept is controlled by the kinetic fractionation occurring during non-equilibrium processes such as evaporation (Craig 1961; Cappa *et al.* 2003). The intercept parameter, d ($= \delta\text{D} - 8\delta^{18}\text{O}$), termed as deuterium excess, provides information on the climatic conditions at the oceanic source region, but can be modified by the vapour evaporated in continental basins (Aragus-Aragus *et al.* 2000).

The deuterium excess, obtained for the three regions in the Pamba basin, ranged between 11.5 and 25.4‰ in the lowlands; between 11.8 and 25.6‰ in the midlands and between 15.9 and 28.2‰ in the highland (table 1). The standard deviation was found to be similar for the three regions. The variation of seasonally averaged d-excess values in the lowland, midland and highland regions of the basin is provided in figure 7. A closer look at the distribution of d-excess in the basin reveals that the values were consistently higher than 10‰, at all locations in three seasons.

When evaporation takes place from a water body, the d-excess value of the residual water lowers and the evolving vapour will have a higher d-excess. The precipitation formed by the condensation of such vapour will also have a high d-excess (Clark and Fritz 1997). Seasonal variation of d-excess of the Pamba River basin also exemplifies this. During the pre-monsoon period, high surface air temperature and low RH facilitate evaporation from the land surfaces, and the vapour formed may have a high d-excess. This fraction of vapour has a clear influence on the precipitation occurring in this season. During the monsoon season, evaporation is negligible, and as a consequence, the d-excess also gets lowered.

Moreover, deuterium excess is related to humidity and temperature at the moisture source

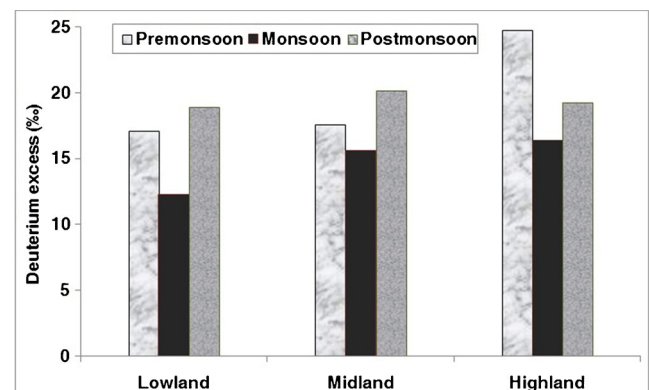


Figure 7. Seasonal variation of deuterium excess in the Pamba River basin.

(Dansgaard 1964; Merlivat and Jouzel 1979). When evaporation from ocean surface takes place at RH around 85%, the deuterium excess will be around 10‰. If the RH at the vapour source region is less than this value, the d-excess will increase. In other words, the oceanic vapour will have d-excess of 10‰ while the continental vapour, as a result of the difference in RH and rainout history, will have a higher d-excess value. The Pamba River basin experiences two monsoons; the south-west, which is of oceanic origin and the other, north-east, which is of continental origin. The post-monsoon or the north-east monsoon will be carrying vapour from the northern plains of India, which has a significant amount of continental vapour; the d-excess of the precipitation formed from this air mass is high. The seasonal variation in d-excess can be attributed to the different moisture sources in the south-west (14.7‰) and north-east monsoons (19.4‰) and the influence of recycled vapour in the pre-monsoon period.

Further, d-excess was highest in the highland, in the pre-monsoon (24.8‰), and lowest during the monsoon season (16.4‰). As we have seen earlier, the area is covered by dense forests, open forests, plantation crops and supports large reservoirs. Evaporation from the reservoirs and evapotranspiration from the forests may have contributed to the ambient vapour during the pre-monsoon season, increasing the d-excess value. In the lowland and midland regions also, the lowest d-excess was obtained during the monsoon (12.3 and 15.6‰, respectively). However, relatively high values were obtained during the post-monsoon season, in contrast to the highlands. The difference in the origin of vapour sources can be attributed here, also. The lowland region of the study area contains large surface water bodies and many parts are submerged for paddy cultivation. In the midland region, rubber is the main plantation crop followed by coconut, pepper, banana, etc. Earlier studies have shown that rubber acts as ‘water pumps’ drawing a considerable amount of soil moisture and transpiring (Gourdiola-Claramonte *et al.* 2008; Fox *et al.* 2014; Celine and James 2015). Vapour formed by the evaporation of surface water bodies and irrigated water in the pre-monsoon, which has higher d-excess values, may have influenced the stable isotopic composition of the ambient vapour. In general, the influence of recycled vapour can be seen in the study area, even though it is situated in the humid tropical climate.

3.5 The Rayleigh distillation model

As we have seen earlier, the isotopic composition of precipitation occurring at a particular location

Table 4. Isotope abundance ratios and the fraction of air mass remaining in the three regions of the Pamba River Basin as obtained from the precipitation δ values.

	$\delta^{18}\text{O}$	R	F
Lowland (P1)	-4.60	0.001995	0.76
Midland (P2)	-4.84	0.001994	0.74
Highland (P3)	-6.06	0.001992	0.64
All rain	-5.16	0.001994	0.71

is a product of several stages of fractionation processes starting from the evaporation of water from the oceans till the in-cloud condensation processes. Further partitioning of heavier isotopes between different phases is caused during rainout by the Rayleigh distillation process (Craig 1961). Along the trajectory of air masses, each rainout distills the heavy isotopes from the vapour. Therefore, in the rainout process, not only does the vapour mass decrease progressively, but the remaining vapour also becomes progressively depleted in heavier isotopes. Thus the isotopic evolution during rainout can be modelled according to the Rayleigh distillation equation (Clark and Fritz 1997). The equation is given below.

$$R = R_0 f^{\alpha-1},$$

where R_0 is the initial isotope ratio of the precipitation vapour and R represents the isotope ratio after a given proportion of the vapour has rained out. The residual vapour reservoir fraction is denoted by f and α is the equilibrium fractionation factor for the water–vapour system.

In this study, from the intersection point of the LMWL with the GMWL, the initial isotopic composition of precipitation is deduced as follows: $\delta\text{D} = -6\text{‰}$ and $\delta^{18}\text{O} = -2\text{‰}$. The isotopic abundance ratios were computed from the δ values and the fraction ‘ f ’ of the remaining vapour was calculated and given in table 4 for the different regions.

The arithmetic mean of the δ values of precipitation collected in different months for each location was used for this study. From the computations, it can be seen that around 75% vapour remains in the air mass, in the lowland and midland regions. As with the progressive depletion of heavier isotopes from the lowland to the highland, the vapour is also found to be decreasing from 76 to 64%. If all the rains are considered together, we can say, about 30% of vapour in the original air mass is raining out in the Pamba River basin.

4. Conclusions

The stable isotopes of hydrogen and oxygen in precipitation of a tropical humid river basin, Pamba, in Kerala are probed to find out the spatiotemporal

variation in isotope composition and the vapour sources of precipitation. δD and $\delta^{18}O$ of the monthly composite precipitation samples collected from the lowland (<7 m), midland (7–75 m) and highland (>75 m) regions showed significant seasonal and spatial variation. Altitude effect was manifested well in the study area (0.1‰ for $\delta^{18}O$ and 0.8‰ for δ^2H per 100 m elevation), while the evidence for the amount effect was not clearly visible. The meteorological parameters are more or less similar in the three physiographic regions during south-west monsoon and the wind direction is uniform from the surface up to 6 km and the wind speed is up to 60 kt. The precipitation may have formed from the marine moisture, which is supplied at a steady rate, without much isotopic evolution in this period masking the possible depletion of heavier isotopes with increasing rainfall. The precipitation in the lowland and midland regions can be considered as the first condensate of the monsoon vapour and the precipitation occurring in the highlands showed rainout evolution. Contribution from locally recycled vapour in precipitation of the area can be deduced from high d-excess values, particularly in the pre-monsoon season. The local meteoric water line developed for the basin showed evaporative enrichment and the fraction of rain precipitated was calculated to be ~30% from the Rayleigh distillation model.

Acknowledgements

The authors are indebted to the Department of Science and Technology, Government of India for establishing the 'National Stable Isotope Facility for Research in Basic and Applied Science' at CWRDM with which we could carry out this programme. We are also grateful to the Chief Engineer, Kerala State Electricity Board; Dr Geetha Gopinath, Principal, Mar Thoma Teachers Training College, Pathanamthitta and the authorities of the Vattapayithra Temple, Alappuzha, for facilitating precipitation sample collection. Thanks are also due to the Directors of the Kerala Agricultural University Rice Research Station at Mancompu, and Sugarcane Research Station, Thiruvalla, for providing the climate data. We thank Prof. K V Jayakumar, former Executive Director, CWRDM, for permitting to carry out this study. We are also thankful to Dr N B Narasimha Prasad, Executive Director, CWRDM, for permitting to publish this paper.

References

- Aragus-Aragus L, Froehlich K and Rozanski K 2000 Deuterium and oxygen-18 isotopic composition of precipitation and atmospheric moisture; *Hydrol. Process.* **14** 1344–1355.
- Brietenbach S F M, Adkins J F, Meyar H, Marwan M, Kumar K K and Haug G H 2010 Strong influence of water vapour source dynamics on stable isotopes in precipitation observed in southern Meghalaya, NE India; *Earth Planet. Sci. Lett.* **292** 212–220.
- Cappa C D, Hendricks M B, DePaolo D J and Cohen R C 2003 Isotopic fractionation of water during evaporation; *J. Geophys. Res.* **108**(D16) 4522–4534.
- Celine G and James E J 2015 Assessing the implications of extension of rubber plantation on the hydrology of humid tropical river basin; *Int. J. Environ. Res.* **9**(3) 841–852.
- Chattopadhyay S 2015 *Environmental consequences of rubber plantations in Kerala*; NRPPD Discussion Paper 44, pp. 10–11.
- Clark I D and Fritz P 1997 *Environmental isotopes in hydrogeology*; Lewis/CRC Press.
- Cortés A, Durazo J and Farvolden R N 1997 Study of isotope hydrology of the basin of Mexico and vicinity: Annotated bibliography and interpretation; *J. Hydrol.* **198** 346–376.
- Craig H 1961 Isotope variations in meteoric waters; *Science* **133**(3465) 1702–1703.
- Croucher P 2007 *Professional helicopter pilot studies*; pp. 8–28.
- CWC 2006 *Integrated hydrological data book*; Central Water Commission, New Delhi, 29p.
- CWRDM 1995 *Water Atlas of Kerala*; 9p.
- Dansgaard W 1964 Stable isotopes in precipitation; *Tellus* **XVI**(4) 436–468.
- Deshpande R D, Bhattacharya S K, Jani R A and Gupta S K 2003 Distribution of oxygen and hydrogen isotopes in shallow groundwaters from southern India: Influence of a dual monsoon system; *J. Hydrol.* **271** 226–239.
- Epstein S and Mayeda T 1953 Variation of the O^{18} content of waters from natural sources; *Geochim. Cosmochim. Acta* **4** 213–224.
- Forstel H 1982 $^{18}O/^{16}O$ ratio of water in plants and their environment; In: *Stable Isotopes* (eds) Schmidt H L, Forstel H, and Heizinger K J, Elsevier, Amsterdam, The Netherlands, pp. 503–516.
- Fox J M, Castella J-C, Ziegler A D and Westley S B 2014 Rubber plantations expand in mountainous southeast Asia: What are the consequences for the environments; East West Center, *Asia Pacific Issues* **114** 1–8.
- Fritz P and Fontes J Ch 1986 Isotopes in cloud physics: Multiphase and multistage condensation process; In: *Handbook of Environmental Isotope Geochemistry. Volume 2, the Terrestrial Environment* (eds) Fritz P and Fontes J Ch, Elsevier, Amsterdam, The Netherlands, pp. 71–73.
- Gammons C H, Poulson S R, Pellicori D A, Reed P J, Roesler A J and Petersue E M 2006 The hydrogen and oxygen isotopic composition of precipitation, evaporated mine water, and river water in Montana, USA; *J. Hydrol.* **328** 319–330.
- García M, Villalba F, Aragus-Aragus L and Rozanski K 1998 The role of atmospheric circulation patterns in controlling the regional distribution of stable isotope contents in precipitation: Preliminary results from two transects in Ecuadorian Andes, In: *Isotope Techniques in the Study of Environmental Change*; IAEA, Vienna, pp. 127–140.
- Gonfiantini R, Roche M-A, Olivry J-Cl, Fontes J-Ch and Zuppi G M 2001 The altitude effect on the isotopic composition of tropical rains; *Chem. Geol.* **181** 147–167.
- Gopakumar R and Takara K 2009 Water balance and mean water residence time of the Vembanad Wetland of Kerala State, India; In: *Ecohydrology of surface and*

- groundwater dependent systems: Concepts, methods and recent developments, *IAHS Publ.* **328** 223–232.
- Gordon L J, Steffen W, Jonsson B F, Folkem C, Falkenmark M and Johannessen A 2005 Human modification of global water vapor flows from the land surface; *Proc. Natl. Acad. Sci. USA* **102** 7611–7617.
- Gourdiola-Claramonte M, Troch P A, Ziegler A D, Giambelluca T W, Vogler J B and Nullet M A 2008 Local hydrological effects of introducing non-native vegetation in a tropical catchment; *Ecohydrology* **1** 13–22.
- Guan H, Simmons G T and Love A J 2009 Orographic controls of rain water isotope distribution in the Mount Lofty Ranges of South Australia; *J. Hydrol.* **374** 255–264.
- Gupta S K and Deshpande R D 2003 Synoptic hydrology of India from the data of isotopes in precipitation; *Curr. Sci.* **85(11)** 1591–1595.
- Gupta S K and Deshpande R D 2005 Groundwater isotopic investigations in India: What has been learned? *Curr. Sci.* **89(5)** 825–835.
- Gupta S K, Deshpande R D, Bhattacharya S K and Jani R A 2005 Groundwater $\delta^{18}\text{O}$ and δD from central Indian peninsula: Influence of the Arabian Sea and the Bay of Bengal branches of the summer monsoon; *J. Hydrol.* **303** 38–55.
- Hu C, Froehlich K, Zhou P, Lou Q, Zeng S and Zhou W 2013 Seasonal variation of oxygen-18 in precipitation and surface water of the Poyang Lake Basin, China; *Isot. Environ. Health. S* **49(2)** 188–196.
- Hunjak T, Lutz H O and Roller-Lutz Z 2013 Stable isotope composition of the meteoric precipitation in Croatia; *Isot. Environ. Health. S* **49(3)** 336–345.
- James M E 1991 Studies on space-time variabilities of hydrometeorological parameters over Kerala State; Thesis submitted to the Cochin University of Science and Technology, Kochi, India.
- Kattan Z 2006 Characterization of surface water and groundwater in the Damascus Ghotta Basin: Hydrochemical and environmental isotope approaches; *Environ. Geol.* **51** 173–201.
- Kumar U S, Kumar B, Rai S P and Sharma S 2010 Stable isotope ratios in precipitation and their relationship with meteorological conditions in the Kumaon Himalayas, India; *J. Hydrol.* **391** 1–8.
- Madhusoodhanan C G, Putty M R Y and Eldho T I 2012 Assessment of basin yield for the Western Ghats rivers of Kerala, *Proceedings of the National Conference on Hydraulics & Water Resources*; SVNIT, Surat, India, pp. 152–161.
- Mayaja N A and Srinivasa C V 2014 Rainfall characteristics of Pampa river basin, Kerala: A time series analysis; *Int. J. Innov. Res. Adv. Eng.* **1(8)** 363–370.
- Menon P A and Rajan C K 1989 *Climate of Kerala*; Classic Publishing House, Cochin.
- Merlivat L and Jouzel J 1979 Global climatic interpretation of the deuterium-oxygen-18 relationship for precipitation; *J. Geophys. Res.* **84** 5029–5033.
- NWDA 2008 Feasibility Report of Pamba Achankovil Vaippar Link; National Water Development Agency, Government of India.
- Peng T R, Wang C H, Huang C C, Fei L Y, Chen C T A and Hwong J L 2010 Stable isotopic characterization of Taiwan's precipitation: A case study of western Pacific monsoon region; *Earth Planet. Sci. Lett.* **289** 357–366.
- Pradeep Kumar P K 1994 Physiographic features and changes in rainfall pattern of Kerala; Ph.D. thesis submitted to Cochin University of Science and Technology, Kochi, India.
- Rhodes A L, Guswa A J and Newell S E 2000 Seasonal variation in the stable isotopic composition of precipitation in the tropical montane forests of Monteverde, Costa Rica; *Water Resour. Res.* **42** W11402.
- Rozanski K, Araguas-Araguas L and Gonfiantini R 1993 Isotopic patterns in modern global precipitation; In: *Climate change in continental isotopic records* (eds) Swart P K, Lohmann K L, McKenzie J and Savin S, American Geophysical Union, Washington DC, pp. 1–37.
- Rozanski K, Sonntag G and Munnich K O 1982 Factors controlling stable isotope composition of European precipitation; *Tellus* **34** 142–150.
- Saravanan E 1994 Agroclimatological studies of Kerala state for application in land use planning; Ph.D. thesis submitted to the Cochin University of Science and Technology, Kochi, India.
- Schmidt G A, Le Grande A N and Hoffmann G 2007 Water isotope expressions of intrinsic and forced variability in a coupled ocean-atmosphere model; *J. Geophys. Res.-Atmos.* **112** D10103.
- Scholl M A, Shanley J B, Zegarra J P and Coplen T B 2009 The stable isotope amount effect: New insights from NEXRAD echotops, Luquillo Mountains, Puerto Rico; *Water Resour. Res.* **45** W12407.
- Simpkins W W 1995 Isotopic composition of precipitation in central Iowa; *J. Hydrol.* **172** 185–207.
- Soman M K and Krishna Kumar K 1993 Space-time evolution of meteorological features associated with the onset of Indian summer monsoon; *Mon. Wea. Rev.* **121** 1177–1194.
- Soman M K, Krishnakumar K and Singh N 1988 Decreasing and trend in the rainfall of Kerala; *Curr. Sci.* **57** 7–12.
- Stumpp C, Klaus J and Stichler W 2014 Analysis of long-term stable isotopic composition in German precipitation; *J. Hydrol.* **517** 351–361.
- Sturm C, Vimeux F and Krinner G 2007 Intraseasonal variability in South America recorded in stable water isotopes; *J. Geophys. Res.* **112** D20118.
- Surendran U, Sushanth C M, Mammen G and Joseph E J 2014 Crop water requirement using FAO-CROPWAT model and assessment of water resources for sustainable water resource management in Kozhikode district of humid tropical Kerala, India; *Proc. Int. Sympos. Integr. Water Resour. Manag.* **2** 894–902.
- Vreča P, Bronić I K, Horvatinčić N and Barešić J 2006 Isotopic characterization of precipitation in Slovenia and Croatia: Comparison of continental and maritime stations; *J. Hydrol.* **330** 457–469.
- Vuille M, Werner M, Bradley R S and Keiming F 2005 Stable isotopes in precipitation in the Asian monsoon region; *J. Geophys. Res.* **110** D23108.
- Warrier C U, Praveenbabu M, Manjula P, Velayudhan K T, Shahul Hameed A and Vasu K 2010 Isotopic characterization of dual monsoon precipitation – evidence from Kerala, India; *Curr. Sci.* **98(11)** 1487–1495.
- Wassenaar L I, Athanopoulos P and Hendry M J 2011 Isotope hydrology of precipitation, surface and ground waters in the Okanagan Valley, British Columbia, Canada; *J. Hydrol.* **411** 37–48.
- Windhorst D, Waltz T, Timbe E, Frede H-G and Breuer L 2013 Impact of elevation and weather patterns on the isotopic composition of precipitation in a tropical montane rainforest; *Hydrol. Earth Syst. Sci.* **17** 409–419.

Yang Y, Xiao H, Qin Z and Zou S 2013 Hydrogen and oxygen isotopic records in monthly scales variations of hydrological characteristics in the different landscape zones of alpine cold regions; *J. Hydrol.* **499** 124–131.

Zimmerman U, Munnich K O and Roether W 1967 Downward movement of soil moisture traced by means of hydrogen isotopes; In: *Isotope Techniques in the Hydrological Cycle*, Geophysical Monograph Series 11, American Geophysical Union, pp. 28–36.

MS received 4 January 2016; revised 6 July 2016; accepted 25 July 2016

Corresponding editor: SUBIMAL GHOSH